



Parametric optimization and statistical evaluation of a spray dryer for the evaporation of caustic soda solution



B.A. Olufemi^{a,*}, M.K. Ayomoh^b

^a Department of Chemical and Petroleum Engineering, University of Lagos, Lagos, Nigeria

^b Department of Industrial and Systems Engineering, University of Pretoria, 0028, Hatfield, Pretoria, South Africa

ARTICLE INFO

Keywords:
Chemical engineering
Energy

ABSTRACT

Optimum evaporation of a 50% w/w caustic soda solution with a spray dryer was investigated in this work to enhance performance and statistically evaluate process parameters. Application of suitable model with validation, fabrication and operation within predicted optimum values enabled high performance, productivity and energy conservation. The highest exit mass flow rate of NaOH was 0.0459 kg/s, depicting 12% better value than the computed optimum value. The highest value of 73.85% was obtained for the exit final NaOH weight percent. Improvement over conventional multiple effect evaporators to obtain 73% w/w NaOH solution resulted in energy savings of about 2.34×10^6 J/kg (about 99.6565% specific energy savings). Statistical evaluation of process parameters using Analysis of Variance (ANOVA), Bonferroni-Holm, Holm-Sidak and Tukey Posthoc parametric tests enabled the confirmation of significant relationships among operating variables. The outcome indicated the possibility of better attainments in the field.

1. Introduction

Understanding of process variables coordination is necessary for better and efficient operation. Without doubt, the thermal energy demands of the chlor-alkali industry are enormous. The need for possible and affordable means of reducing the cost of these energy needs is an ever-exploring task. Due to process requirements, the initial catholyte product leaving the electrolysis cells in the electrochemical production of caustic soda at various levels of concentration usually requires further evaporation to the sale-able grades of about 73% w/w NaOH and further up to almost 100% anhydrous products. Mostly, high thermal energy consuming multiple effect evaporators are engaged to achieve higher commercial concentrations.

In addition to the high thermal energy demanding processes needed, the materials of construction required are equally expensive which needs replacement periodically due to high temperature operations. Steam usually serves as the source of energy for evaporation. The presence of NaCl in the electrochemical cell liquid products requires that the evaporator should be equipped with scraper blades or other devices to draw

off its precipitates. Approximately, from the catholyte of about 12% w/w caustic solution, the steam needed to make 50% w/w NaOH was given as 2.68×10^6 J/kg NaOH according to Tilak et al. (2007). Worrel et al. (2000) approximately gave 2.35×10^6 J/kg and 3.18×10^6 J/kg of energy as needed to produce 73% w/w and 100% w/w from 50% w/w NaOH solution respectively. Patel (2009) recounted that the chlor-alkali energy cost estimate is about 60–70% of the production cost.

In addition to the conventional multiple effect evaporators, other approaches that have been applied to evaporate caustic soda solution catholytes have been reported (Olufemi et al., 2012a, 2012b). The spray dryer technique is with a view to eliminate most of the limitations in the conventional multiple effect evaporators which ranges from high energy demand, corrosion and expensive replacement of materials leading to intermittent shut-downs. The spray drying technique contacts fine sprays of the solution in moving hot dry air suspended in space without actually touching the dryer walls while varying quantity of moisture removed from the solution feed.

Many researchers had explored the spray dryer operation and characteristics. Tolmac et al. (2011) modeled and experimentally studied flat

* Corresponding author.

E-mail address: bolufemi@unilag.edu.ng (B.A. Olufemi).

air velocity profile and high swirl airflow pattern to dry 55% solution of starch and water with a spray dryer. [Kajiya and Park \(2010\)](#) investigated the influence of air parameters on spray energy consumption. Reactive absorption of CO₂ with NaOH as an absorbent had been experimentally studied on a laboratory scale spray dryer ([Kavoshi et al., 2011](#)). Optimization, scale-up, and design of a commercial-scale spray-drying method in the pharmaceutical industry had been reported ([Dobry et al., 2009](#)). [Djaeni et al. \(2015\)](#), had also presented an energy particulate efficient drying with commendable results in the agro sector.

Optimization of processes and process parameters have been a continuous activity over the years and few recent accounts are given. [Noh et al. \(2018\)](#) have reported an optimization-based strategy for the development of crude selection in a refinery with lube base oil (LBO) producing capability for deciding crude procurement, grade of LBO to be produced and conversion rate in the lube oil process. [Gao et al. \(2018\)](#) also presented application and comparison of derivative-free optimization algorithms to control and optimize free radical polymerization simulated using the kinetic Monte Carlo method. The work resulted in the achievement of synthesis conditions for achieving property targets and minimizing reaction time, advancing design of polymer microstructures and polymerization process control. [Kwak et al. \(2018\)](#) also worked on an energy-efficient design and optimization of boil-off gas (BOG) re-liquefaction process for liquefied natural gas (LNG)-fuelled ship. After optimization, sensitivity analysis was also performed to understand how the variation of operating conditions affects on-system performance of BOG re-liquefaction process under different design conditions and constraints. [Ghosh et al. \(2018\)](#) in addition reported parametric optimization of gas metal arc welding process by PCA based Taguchi method on Austenitic Stainless Steel AISI 316L. From the study, optimum parametric settings were predicted and validated. Useful interpretations of the experimental results and subsequent analysis were made to draw some meaningful conclusions.

This present work considered evaporation of 50% w/w caustic soda solution with a fabricated spray dryer using appropriate established process description, modeling, simulation, optimization of important process parameters, coupled with fabrication and parametric operation to achieve highly commendable performance, productivity and energy utilization, with sound statistical evaluation of the significance of process parameters for better and future performance.

2. Materials and methods

2.1. Experimentation

The schematic view of the stainless steel fabricated spray dryer with atomizer is shown in [Fig. 1](#). The dryer is about 1.8 m in height with a diameter of 1m. Inlet solution containing 50% w/w NaOH solution is fed to the top of the spray dryer through a solution feed pipe. The dryer operates at atmospheric pressure. The rotary atomizer generates feed solution fine sprays as shown, and flows counter-currently against up-coming hot dry air from the base. The colder wet air flows out at the top through the cold wet air outlet pipe, while the evaporated NaOH solution product is collected at the base of the dryer. Varying operating regulated inlet air temperatures of 373, 382 and 391 K were used with various inlet NaOH mass flow rates of 0.0115, 0.0179, 0.0303, 0.0488, 0.0490, 0.0599 and 0.066 kg/s. The heater was rated with a maximum capacity of 3 kW. Parameters monitored and recorded for all runs with the three different inlet air temperatures include outlet air temperature, final NaOH wt.%, final NaOH mass flow rate in kg/s, percent specific energy reduction, specific energy of evaporation in J/kg of NaOH, volume percentage reduction with the ambient temperature (298–307 K). Experimental operating parameters with practicable values near the optimum were implemented throughout the operation of the spray dryer in order to characterize and optimize the drying operation.

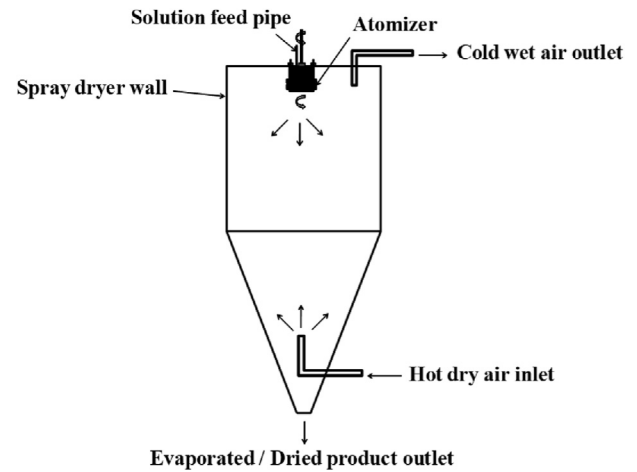


Fig. 1. Schematic view of the atomizing spray dryer.

2.2. Simulation and optimization technique

The validated mathematical modeling with simulation of the typical spray dryer operation based on the mass and energy balance model with appropriate considerations given in [Olufemi et al. \(2012a\)](#) predicts the drying operation in great details. For productivity and energy optimization implementation,

An extensive heat balance around the spray dryer is given as:

$$Q_{IA} + Q_{SI} = Q_{HC} + Q_{DC} + Q_{SR} + Q_{OA} + Q_{SO} + Q_{WO} \quad (1)$$

where,

$$Q_{IA} = \dot{m}_{IA} C_{pIA} T_{IA} \quad (2)$$

$$Q_{SI} = \dot{m}_C C_{pC} T_{IA} \quad (3)$$

$$Q_{HC} = \dot{m}_C C_{pC} (T_{IA} - T_C) \quad (4)$$

where the mean dryer temperature

$$T_{MA} = \frac{T_{OA} + T_{IA}}{2} \quad (5)$$

$$Q_{DC} = \dot{m}_C \lambda_C \quad (6)$$

$$Q_{SR} = h_A A_W (T_{MA} - T_{SR}) \quad (7)$$

$$A_W = \pi D_I l \quad (8)$$

$$Q_{OA} = \dot{m}_{OA} C_{pOA} T_{OA} \quad (9)$$

$$Q_{SO} = \dot{m}_C C_{pC} T_{OA} \quad (10)$$

$$Q_{WO} = \dot{m}_{WO} C_{pWO} T_{OA} \quad (11)$$

But

$$\dot{m}_{WO} = \dot{m}_C - \dot{m}_{CF} \quad (12)$$

Substituting Eqs. (2), (3), (4), (5), (6), (7), (8), (9), (10), (11), and (12) into Eq. (1), rearranging, and re-writing $\dot{m}_{CF} = \frac{dm_{CF}}{dt}$, which represents the rate of change of the final mass flow rate of the solution being dried per time,

$$\frac{dm_{CF}}{dt} = \frac{[m_{IA}C_{pIA}T_{IA} + m_c(C_{PC}T_C - C_{PC}T_{MA} - \lambda_C - C_{PWO}T_{OA}) - h_A A_w(T_{IA} - T_{SR}) - m_{OA}C_{POA}T_{OA}]}{C_{PC}T_{CF} - C_{PWO}T_{OA}} \quad (13)$$

Eq. (13) is the expression of the final mass flow rate of the dried solution from the spray dryer after drying, which indicates the objective function for product maximization.

The volume percentage reduction after drying is given as:

$$V_r = \frac{(V_i - V_f)}{V_i} \quad (14)$$

The specific energy supplied for evaporation in (J/kg NaOH) is given as:

$$Q_{SP} = \frac{(Q_{IA} + Q_{SI} - Q_{OA})}{\dot{m}_c} \quad (15)$$

The heat transfer coefficient of air is evaluated by the method of McCabe et al. (2001) also adopted by Olufemi et al. (2012a) as follows:

$$h_A = [k_{AR}b(Gr.Pr)^n]/l \quad (16)$$

where the Grashof number (Gr) of the surrounding air is given as:

$$Gr = \frac{\hat{\rho}^2 \rho_{AR}^2 g \beta_{AR} (T_W - T_{SR})}{\mu_{AR}^2} = \frac{\hat{\rho}^2 \rho_{AR}^2 g \left(\frac{1/\rho_2 - 1/\rho_1}{(T_{IO} - T_{SR}) \left(\frac{1/\rho_1 + 1/\rho_2}{2} \right)} \right) (T_W - T_{SR})}{\mu_{AR}^2} \quad (17)$$

ρ_1 = density of air at T_{SR} (kgm^{-3})
 ρ_2 = density of air at T_W (kgm^{-3})

$$Pr = \frac{C_{PA} \mu_{AR}}{k_{AR}} \quad (18)$$

Air properties κ_{AR} , μ_{AR} , C_{PA} and ρ_{AR} were evaluated at the mean film temperature, T_{fm} , given as:

$$T_{fm} = \frac{T_W + T_{SR}}{2} \quad (19)$$

and

$$T_w = \frac{T_{MA} + T_{SR}}{2} \quad (20)$$

The constants b and n in Eq. (16) are estimated as follows:

$b = 0.59$ if $10^4 < (Gr \bullet Pr) < 10^9$, $b = 0.13$ if $10^9 < (Gr \bullet Pr) < 10^{12}$
 $n = 0.25$ if $10^4 < (Gr \bullet Pr) < 10^9$, $n = 0.333$ if $10^9 < (Gr \bullet Pr) < 10^{12}$

The Grashof number (Gr) of the surrounding air is given as:

$$Gr = \frac{\hat{\rho}^2 \rho_{AR}^2 g \beta_{AR} (T_W - T_{SR})}{\mu_{AR}^2} = \frac{\hat{\rho}^2 \rho_{AR}^2 g \left(\frac{1/\rho_2 - 1/\rho_1}{(T_{IO} - T_{SR}) \left(\frac{1/\rho_1 + 1/\rho_2}{2} \right)} \right) (T_W - T_{SR})}{\mu_{AR}^2} \quad (21)$$

ρ_1 = density of air at T_{SR} (kgm^{-3})
 ρ_2 = density of air at T_W (kgm^{-3})

$$Pr = \frac{C_{PA} \mu_{AR}}{k_{AR}} \quad (22)$$

Air properties κ_{AR} , μ_{AR} , C_{PA} and ρ_{AR} were evaluated at the mean film temperature, T_{fm} , given as:

$$T_{fm} = \frac{T_W + T_{SR}}{2} \quad (23)$$

and

$$T_w = \frac{T_{MA} + T_{SR}}{2} \quad (24)$$

As a good estimation from Worrel et al. (2000), approximately 2.35×10^6 J/kg and 3.18×10^6 J/kg of energy is required to produce 73% and 100% w/w from 50% w/w NaOH solution respectively. For the purpose of performance comparison, the percent specific energy reduction (P_{SR}) expressed in Eq. (25) was derived to show the approximate relative reduction in the quantity of energy required to produce 73% w/w NaOH solution from 50% w/w NaOH solution.

$$P_{SR} = 100 \times \frac{(2.35 \times 10^6 - Q_{SP})}{2.35 \times 10^6} \quad (25)$$

The equations derived above were used to simulate the experimental operation of the spray dryer. This becomes necessary to establish the validity of the model equations in predicting the dryer operations, as well as for optimization purpose. The non-linear First Order Ordinary Differential Equation (O.D.E) in Eq. (13) that gives final mass flow rate of the solution being dried was solved with the Fourth Order Runge-Kutta method, which was later used to calculate other simulated parameters.

The Fourth Order Runge-Kutta used because of its accuracy (Thomas and Finney, 1984) is described as follows:

For a differential function of mass with respect to time, $f(t) = \dot{m}_{CF} = \frac{dm}{dt}$ at step-wise time interval $h = 0.5$ s, where $0 \leq h \leq 120$ s,

$$k_1 = hf(t, \dot{m}_{CF}) \quad (26)$$

$$k_2 = hf\left(t + \frac{h}{2}, \dot{m}_{CF} + \frac{k_1}{2}\right) \quad (27)$$

$$k_3 = hf\left(t + \frac{h}{2}, \dot{m}_{CF} + \frac{k_2}{2}\right) \quad (28)$$

$$k_4 = hf(t + h, \dot{m}_{CF} + k_3) \quad (29)$$

The new iterative value of the temperature, T_{f+1} can then be calculated as follows:

$$\dot{m}_{CF+1} = \dot{m}_{CF} + \frac{1}{6}(k_1 + 2k_2 + 2k_3 + k_4) \quad (30)$$

The non-linear objective function for the mass flow rate of evaporated caustic soda solution in Eq. (13) was also maximized by observing about thirty-six operational constraints and twelve boundary limits defined by the geometry of the spray dryer, operating conditions and surroundings.

The operational constraints are as follows:

$$T_{IA} \geq T_{OA}, T_{OA} \geq T_{SR}, T_{IA} \geq T_{SR}, T_{IA} \geq T_W, T_{IA} \geq T_C, T_{IA} \geq T_{CF}, T_{IA} \geq T_{MA}, T_{CF} \geq T_C, T_{IA} \geq T_{fm}, T_{MA} = 0.5 T_{IA} + 0.5 T_{OA}, T_W = 0.5 (T_{MA} + T_{SR}), T_{FM} = 0.5 T_{SR} + 0.5 T_W, T_{CF} \geq T_{MA}, T_{MA} \geq T_W, T_{MA} \geq T_{FM}, T_W \geq T_{SR}, T_{MA} \geq T_{SR}, T_{fm} \geq T_{SR}, C_{PIA} = 0.1 T_{IA} + 972.8, C_{POA} = 0.1 T_{OA} + 972.8, C_{PC} + 0.187 T_C = 1846, \lambda_C = 3204 T_{MA} - 65485, (-0.451 T_{OA}^2 + 0.0007836 T_{OA}^3) - 5.201 e^{-7} T_{OA}^4 + C_{PWO} + 116 T_{OA} = 15340, \mu_{AR} = 0.00000004 T_{FM} + 0.000006, \kappa_{AR} = 0.00007 T_{FM} + 0.0046, 0.0025 T_{FM} + \rho_{AR} = 1.95, 0.0025 T_{SR} + \rho_1 = 1.95, 0.0025 T_W + \rho_2 = 1.95, -(1/\rho_2 - 1/\rho_1) / (((T_W - T_{SR}) (1/\rho_1 + 1/\rho_2)) / 2) + \beta_{AR} = 0, -(0.0001 T_{fm} + 0.9728) * \mu_{AR} / \kappa_{AR} + Pr = 0, C_{PC} + 0.187 T_{MA} = 1846, 0.187 T_{CF} +$$

$$C_{PC} = 1846, \dot{m}_{IA} \geq \dot{m}_{OA}$$

The twelve boundary limits are as defined:

$$0.000269 \leq \dot{m}_{IA} \leq 0.000381, 373 \leq T_{IA} \leq 391, 0.008 \leq \dot{m}_C \leq 0.066, 358 \leq T_{MA} \leq 375, 343 \leq T_{OA} \leq 358, 0.225 \leq h_A \leq 1.25666, 298 \leq T_{SR} \leq 307, 328 \leq T_W \leq 337,$$

$$0.000269 \leq \dot{m}_{OA} \leq 0.000381, 298 \leq T_{CF} \leq 391, 313 \leq T_{fm} \leq 318, 298 \leq T_C \leq 307.$$

The non-linear productivity optimization objective function given in Eq. (13) was maximized with the Mathematical Programming Language (MPL) Modelling System, Copyright© 1994–2016, Maximal Software Incorporation Optimization Software.

The software algorithm utilized the Lipschitz-Continuous Global Optimizer (LGO) for the non-linear optimization. As mentioned by Pinter (2007), a practically important point to emphasize is that a specialized model structure is not assumed or exploited by the LGO optimizer. The LGO does not require analytical derivative information, which means that the solver operations are based exclusively on the computation of the objective and constraint function values at algorithmically selected search points. LGO solves global optimization problems on finite 'box' regions, in the possible presence of additional (general) constraints. In a general form, the global optimization model is given as:

$$\min f(x) \tag{31}$$

$$g(x) \leq 0 \tag{32}$$

$$a \leq x \leq b. \tag{33}$$

where,

x is a real n-vector that describes the possible decisions

a, b are finite, component-wise vector bounds regarding x

f(x) is a continuous function that defines the model objective

g(x) is a continuous m-vector function that defines the model constraints; the corresponding vector inequality is interpreted component-wise.

In the ANOVA analysis, the sum of Sums of Squares (SS) is given as:

$$SS_T = \sum_{j=1}^p \sum_{i=1}^{n_j} (x_{ij} - \bar{x})^2 \tag{34}$$

$$SS_B = \sum_{j=1}^p n_j (\bar{x}_j - \bar{x})^2 \tag{35}$$

$$SS_W = \sum_{j=1}^p \sum_{i=1}^{n_j} (x_{ij} - \bar{x}_j)^2 \tag{36}$$

where SS_T , SS_B and SS_W are the total sum of squares, sum of squares between and sum of squares within the groups respectively. The elements of the groups i and j are x, while \bar{x}_j and \bar{x} are the groups and total means respectively. The Mean Squares (MS) is given as:

$$MS_B = \frac{SS_B}{DF_B} \tag{37}$$

$$MS_W = \frac{SS_W}{DF_W} \tag{38}$$

where MS_B and MS_W are the mean squares between and within the groups respectively. The degrees of freedom (DF) between and within the groups are given as DF_B and DF_W respectively.

The Fisher's F is given as:

$$F = \frac{MS_B}{MS_W} \tag{39}$$

3. Results and discussion

The simulated mass flow rate of caustic soda in Eq. (13) using the Fourth Order Runge Kutta method was implemented on a MATLAB software program version 7.9.0.529 (R2009b). In addition, the non-linear productivity optimization objective function given in Eq. (13) was maximized with the Mathematical Programming Language (MPL) Modelling System, Copyright© 1994–2016, Maximal Software Incorporation Optimization Software. All the analysis of variance (ANOVA), Bonferroni-Holm, Holm-Sidak and Tukey Posthoc parametric tests statistical computation were carried out with the aid of the Daniel's XL Toolbox, Version 6.70, Copyright© 2008–2018 Software. The dependence and inter-relationship as well as useful observation from various parameters in the dryer operation were justified statistically as presented.

The simulated data were presented with continuous and dashed lines, while the experimental data were presented with markers alone as shown in Figs. 2, 3, 4, 5, 6, 7, and 8. The model validation of the experimental data has a high level of accuracy. The lowest and highest percentage deviation of simulated from the experimental data was -0.22 and +9.30% respectively.

From the results generated with the MPL LGO software, a parsing time of 3.46 s was required, number of iterations required before convergence was 15,572,820, a solution time of 17 min, 57 s was required and a global solution for the theoretical optimum exit mass flow rate of evaporated caustic soda solution \dot{m}_{CF} was 0.040933 kg/s.

The optimum values of various operational parameters are:

$$\begin{aligned} \dot{m}_{IA} &= 0.000269 \text{ kg/s}, C_{PIA} = 1011.90 \text{ J/kgK}, T_{IA} = 391.0 \text{ K}, \dot{m}_C = 0.066 \text{ kg/s}, \\ C_{PC} &= 1790.27 \text{ J/kgK at } T_C, C_{PC} = 1775.97 \text{ J/kgK at } T_{MA}, T_{MA} = 374.5 \text{ K}, \\ \lambda_C &= 1134413.0 \text{ J/kg}, C_{PWO} = 4203.44 \text{ J/kgK}, T_{OA} = 358.0 \text{ K}, h_A = 0.2250 \text{ W/m}^2\text{K}, \\ T_{SR} &= 299.17 \text{ K}, \dot{m}_{OA} = 0.000269 \text{ kg/s}, C_{POA} = 1008.60 \text{ J/kgK}, T_{CF} = 391.0 \text{ K}, \\ T_{fm} &= 318.0 \text{ K}, T_W = 336.83 \text{ K}, T_C = 298.0 \text{ K}, C_{PC} = 1772.88 \text{ J/kgK at } T_{CF}, \\ \mu_{AR} &= 0.000019 \text{ kg/ms}, \kappa_{AR} = 0.026860 \text{ W/mK}, \rho_{AR} = 1.1550 \text{ kg/m}^3, \\ \rho_1 &= 1.2021 \text{ kg/m}^3, \rho_2 = 1.1079 \text{ kg/m}^3, \beta_{AR} = 0.002165 \text{ K}^{-1}, Pr = 0.0007 \end{aligned}$$

Evidently, there existed a significantly statistically variation among all the parameters investigated for the three inlet air temperatures at the 95% confidence interval. The Fisher's F, which is the ratio of the variance between groups to the variance within groups, had values of 11.614, 11.841 and 11.212 for drying operations at inlet air temperatures of 373, 382 and 391 K respectively. The probability factor P that must be less

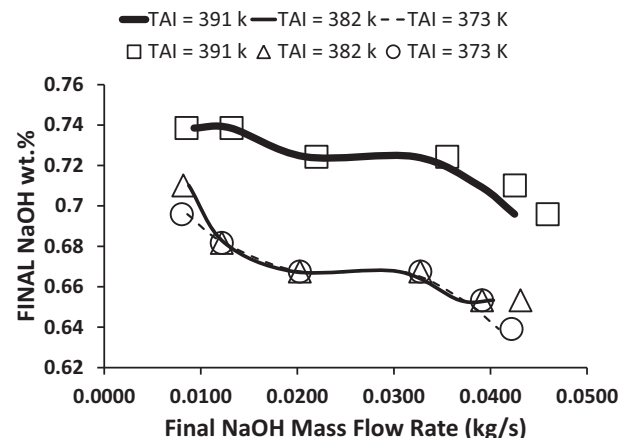


Fig. 2. Variation of Final NaOH wt.% with Final NaOH Mass Flow Rate.

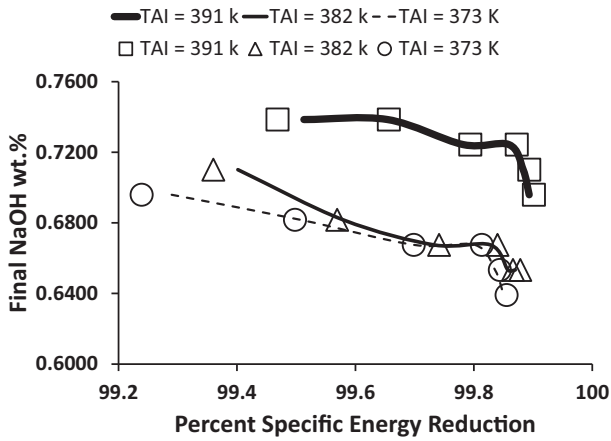


Fig. 3. Variation of Final NaOH wt. % with Percent Specific Energy Reduction.

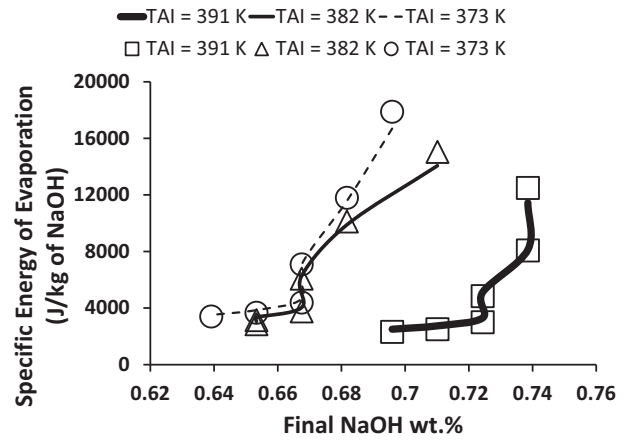


Fig. 6. Variation of Specific Energy of Evaporation with Final NaOH wt. %.

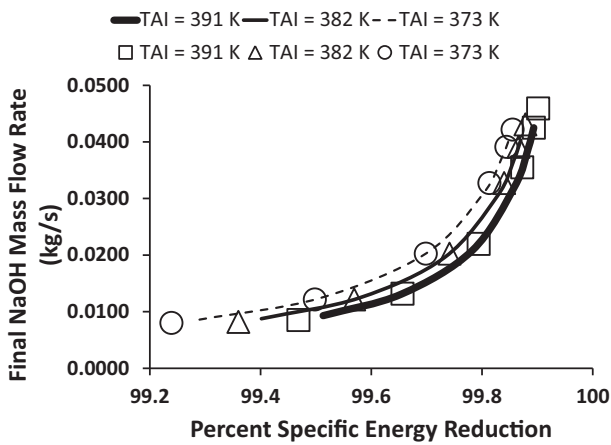


Fig. 4. Variation of final NaOH mass flow rate with percent specific energy reduction.

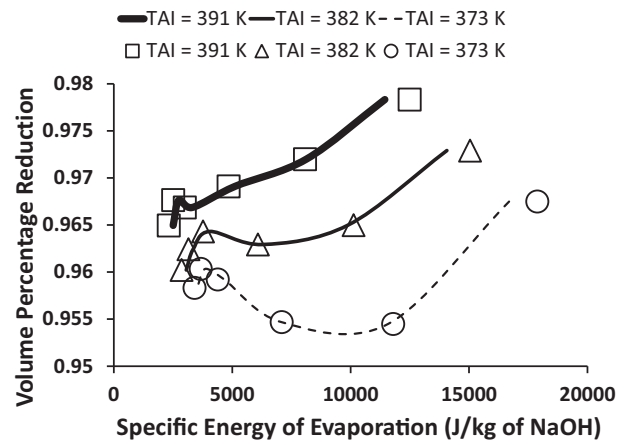


Fig. 7. Variation of volume percentage reduction with specific energy of evaporation.

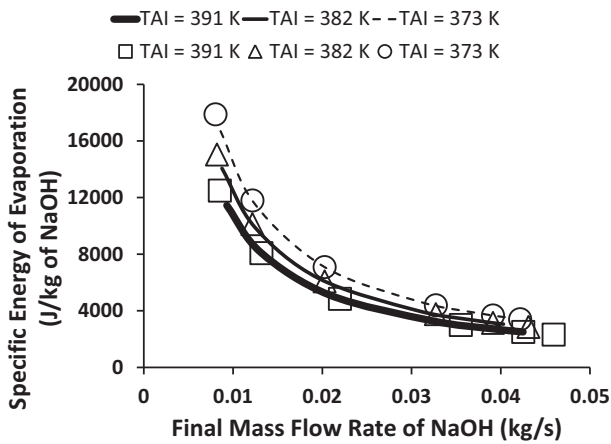


Fig. 5. Variation of specific energy of evaporation with final NaOH mass flow rate.

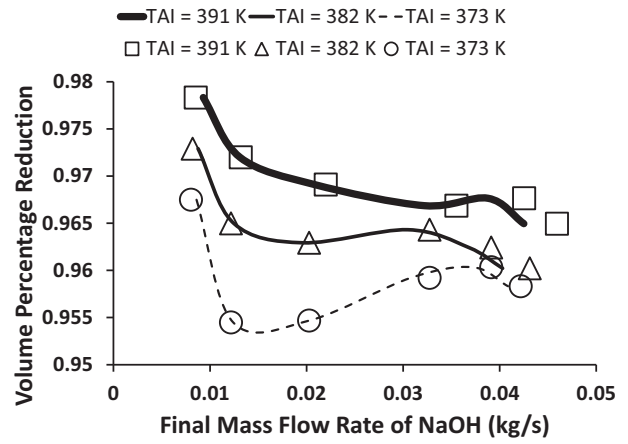


Fig. 8. Variation of volume percentage reduction with final NaOH mass flow rate.

than 0.05 in the 95% confidence interval was less than 1.82E-05, 1.56E-05 and 2.39E-05 for drying operations at 373, 382 and 391 K respectively in the ANOVA analysis. The F and P values implied a strong dependence of Final Mass Flow Rate of NaOH, Final NaOH wt.%, Percent Specific Energy Reduction, Specific Energy of Evaporation and Volume Percentage Reduction among themselves at the three inlet air temperatures of 373, 382 and 391 K. The degree of freedom between the groups was four,

while the degree of freedom within the groups was 25.

As given in Tables 1, 2, 3, 4, 5, and 6, the Bonferroni-Holm, Holm-Sidak and Tukey Posthoc parametric tests for the various parameters were presented at the three operating temperatures, which showed the significance of the various parameters as far as the drying operation is concerned. The Bonferroni-Holm and Holm-Sidak post hoc tests reported

Table 1

Bonferroni-Holm and Holm-Sidak Posthoc parametric tests for final mass flow rate of NaOH, final NaOH wt.%, percent specific energy reduction, specific energy of evaporation and volume percentage reduction at 373 K.

Data Group 1	Data Group 2	Critical P Value	Actual P value
Final Mass Flow Rate of NaOH (kg/s)	Percent Specific Energy Reduction	0.005000	2.61E-26
Volume Percentage Reduction	Percent Specific Energy Reduction	0.005556	2.82E-26
Final NaOH wt.%	Percent Specific Energy Reduction	0.006250	2.83E-26
Volume Percentage Reduction	Final Mass Flow Rate of NaOH (kg/s)	0.007143	3.87E-18
Final NaOH wt.%	Final Mass Flow Rate of NaOH (kg/s)	0.008333	2.2E-14
Volume Percentage Reduction	Final NaOH wt.%	0.010000	9.63E-12
Specific Energy of Evaporation (J/kg NaOH)	Final Mass Flow Rate of NaOH (kg/s)	0.012500	0.006564
Specific Energy of Evaporation (J/kg NaOH)	Final NaOH wt.%	0.016667	0.006567
Specific Energy of Evaporation (J/kg NaOH)	Volume Percentage Reduction	0.025000	0.006569
Specific Energy of Evaporation (J/kg NaOH)	Percent Specific Energy Reduction	0.050000	0.007049

Table 2

Bonferroni-Holm and Holm-Sidak Posthoc parametric tests for final mass flow rate of NaOH, final NaOH wt.%, percent specific energy reduction, specific energy of evaporation and volume percentage reduction at 382 K.

Data Group 1	Data Group 2	Critical P Value	Actual P value
Final Mass Flow Rate of NaOH (kg/s)	Percent Specific Energy Reduction	0.005000	4.68E-27
Volume Percentage Reduction	Percent Specific Energy Reduction	0.005556	5.03E-27
Final NaOH wt.%	Percent Specific Energy Reduction	0.006250	5.14E-27
Volume Percentage Reduction	Final Mass Flow Rate of NaOH (kg/s)	0.007143	3.79E-18
Final NaOH wt.%	Final Mass Flow Rate of NaOH (kg/s)	0.008333	3.26E-14
Volume Percentage Reduction	Final NaOH wt.%	0.010000	1.63E-11
Specific Energy of Evaporation (J/kg NaOH)	Final Mass Flow Rate of NaOH (kg/s)	0.012500	0.006189
Specific Energy of Evaporation (J/kg NaOH)	Final NaOH wt.%	0.016667	0.006192
Specific Energy of Evaporation (J/kg NaOH)	Volume Percentage Reduction	0.025000	0.006194
Specific Energy of Evaporation (J/kg NaOH)	Percent Specific Energy Reduction	0.050000	0.006734

same significance of variables and were reported together in Tables 1, 2, and 3. The Tukey post hoc test however is the least conservative of the three, which is the one most likely to detect significant differences in multiple comparisons. The q-statistic studentized values are also given to give multiple significance testing across the means. As revealed in Tables 1, 2, 3, 4, 5, and 6, all the parameters have good significance based on the fact that the actual P values are less than the critical P and q values, confirming that the drying operating variables represented a good relationship among each other.

For all the drying operations, the maximum and minimum values of some important parameters at the three inlet air temperatures of 373,

Table 3

Bonferroni-Holm and Holm-Sidak Posthoc parametric tests for final mass flow rate of NaOH, final NaOH wt.%, percent specific energy reduction, specific energy of evaporation and volume percentage reduction at 391 K.

Data Group 1	Data Group 2	Critical P Value	Actual P value
Final Mass Flow Rate of NaOH (kg/s)	Percent Specific Energy Reduction	0.005000	7.51E-28
Volume Percentage Reduction	Percent Specific Energy Reduction	0.005556	7.95E-28
Final NaOH wt.%	Percent Specific Energy Reduction	0.006250	8.09E-28
Volume Percentage Reduction	Final Mass Flow Rate of NaOH (kg/s)	0.007143	7.9E-18
Final NaOH wt.%	Final Mass Flow Rate of NaOH (kg/s)	0.008333	4.62E-15
Volume Percentage Reduction	Final NaOH wt.%	0.010000	8.28E-12
Specific Energy of Evaporation (J/kg NaOH)	Final Mass Flow Rate of NaOH (kg/s)	0.012500	0.007203
Specific Energy of Evaporation (J/kg NaOH)	Final NaOH wt.%	0.016667	0.007208
Specific Energy of Evaporation (J/kg NaOH)	Volume Percentage Reduction	0.025000	0.00721
Specific Energy of Evaporation (J/kg NaOH)	Percent Specific Energy Reduction	0.050000	0.007977

Table 4

Tukey Posthoc parametric tests for final mass flow rate of NaOH, Final NaOH wt.%, percent specific energy reduction, specific energy of evaporation and volume percentage reduction at 373 K.

Data Group 1	Data Group 2	q value	Actual P value
Specific Energy of Evaporation (J/kg NaOH)	Final Mass Flow Rate of NaOH (kg/s)	7.64393	0.000211
Specific Energy of Evaporation (J/kg NaOH)	Final NaOH wt.%	7.64332	0.000211
Specific Energy of Evaporation (J/kg NaOH)	Volume Percentage Reduction	7.643042	0.000211
Specific Energy of Evaporation (J/kg NaOH)	Percent Specific Energy Reduction	7.549176	0.00024

Table 5

Tukey Posthoc parametric tests for final mass flow rate of NaOH, final NaOH wt.%, percent specific energy reduction, specific energy of evaporation and volume percentage reduction at 382 K.

Data Group 1	Data Group 2	q value	Actual P value
Specific Energy of Evaporation (J/kg NaOH)	Final Mass Flow Rate of NaOH (kg/s)	7.722514	0.000196
Specific Energy of Evaporation (J/kg NaOH)	Final NaOH wt.%	7.721784	0.000197
Specific Energy of Evaporation (J/kg NaOH)	Volume Percentage Reduction	7.721454	0.000197
Specific Energy of Evaporation (J/kg NaOH)	Percent Specific Energy Reduction	7.609908	0.000218

382 and 391 K are as presented in Table 7.

3.1. Variation of final NaOH weight percent with final NaOH mass flow rate

As shown in Fig. 2, the variation of final NaOH wt.% with final NaOH mass flow rate depicted an inverse relationship, with the wt.% increasing

Table 6

Tukey Posthoc parametric tests for final mass flow rate of NaOH, final NaOH wt.%, percent specific energy reduction, specific energy of evaporation and volume percentage reduction at 391 K.

Data Group 1	Data Group 2	q value	Actual P value
Specific Energy of Evaporation (J/kg NaOH)	Final Mass Flow Rate of NaOH (kg/s)	7.520494	0.000247
Specific Energy of Evaporation (J/kg NaOH)	Final NaOH wt.%	7.519551	0.000247
Specific Energy of Evaporation (J/kg NaOH)	Volume Percentage Reduction	7.519215	0.000247
Specific Energy of Evaporation (J/kg NaOH)	Percent Specific Energy Reduction	7.385047	0.000285

Table 7

Maximum and minimum values of parameters at various inlet air temperatures.

Maximum and Minimum Values of Parameters at Inlet Air Temperature of 373 K		
Parameter	Maximum Value	Minimum Value
Specific Energy of Evaporation (J/kg NaOH)	17882.2746	3403.9150
Volume Percentage Reduction	0.9675	0.9545
Final NaOH wt.%	0.6959	0.6391
Final Mass Flow Rate of NaOH (kg/s)	0.0422	0.0080
Percent Specific Energy Reduction	99.8552	99.2391
Maximum and Minimum Values of Parameters at Inlet Air Temperature of 382 K		
Parameter	Maximum Value	Minimum Value
Specific Energy of Evaporation (J/kg NaOH)	15040.2778	2857.8564
Volume Percentage Reduction	0.9729	0.9602
Final NaOH wt.%	0.7101	0.6533
Final Mass Flow Rate of NaOH (kg/s)	0.0431	0.0082
Percent Specific Energy Reduction	99.8784	99.3600
Maximum and Minimum Values of Parameters at Inlet Air Temperature of 391 K		
Parameter	Maximum Value	Minimum Value
Specific Energy of Evaporation (J/kg NaOH)	12493.4951	2317.7340
Volume Percentage Reduction	0.9783	0.9650
Final NaOH wt.%	0.7385	0.6959
Final Mass Flow Rate of NaOH (kg/s)	0.0459	0.0085
Percent Specific Energy Reduction	99.9014	99.4684

with decreasing mass flow rate. It can also be depicted from the figure that higher temperature of the inlet air favored increase in the weight percent, as the operation at 391 K produced higher final NaOH wt.% than the operation at 382 K, which also produced higher values than those of 373 K. There existed a significantly statistically wide variation between the experimental final NaOH wt.% at various final NaOH mass flow rates and temperatures at the 95% confidence interval, as stated earlier based on the Fisher's F and probability factor P values. As presented in Tables 1, 2, and 3, the Bonferroni-Holm Posthoc parametric tests for the final NaOH wt.% and final NaOH mass flow rates at the three operating temperatures further showed that they are significant.

From Tables 4, 5, and 6, the highest maximum value of the final NaOH wt.% was 0.7385, while the highest maximum final mass flow rate of NaOH was 0.0459 kg/s at an inlet air temperature of 391 K. The lowest minimum value of the final NaOH wt.% was 0.6391, while the lowest minimum value of the final mass flow rate of NaOH was 0.0080 kg/s, which was obtained at an inlet air temperature of 373 K.

3.2. Variation of final NaOH weight percent with percent specific energy reduction

Referring to Fig. 3, the variation of final NaOH wt.% with the percent specific energy reduction is somewhat that of an inverse relationship, with the NaOH wt.% increasing with decreasing percent specific energy reduction. It can in addition be seen from the figure that higher temperature of the inlet air favored increase in the weight percent, as the operation at 391 K produced higher final NaOH wt.% than the operation at 382 K, which also produced higher values than those of 373 K as far as the percent specific energy reduction is concerned.

As stated earlier, there is a justification of a significant statistically wide variation between the experimental final NaOH wt.% for various percent specific energy reduction and inlet air temperatures at the 95% confidence interval, based on the Fisher's F and probability factor P values. The range of values is not just mere replication, but the existence of a relationship. Based on the information in Tables 1, 2, and 3, the Bonferroni-Holm Posthoc parametric tests for the final NaOH wt.% at various percent specific energy reduction at the three operating temperatures further showed that they are significant. The highest maximum value of the percent specific energy reduction was 99.9014 at an inlet air temperature of 391 K, while the lowest minimum value of the percent specific energy reduction was 99.2391, obtained at an inlet air temperature of 373 K as presented in Tables 4, 5, and 6.

3.3. Variation of final NaOH mass flow rate with percent specific energy reduction

As shown in Fig. 4, the variation of the final NaOH mass flow rate with the percent specific energy reduction portrayed that the former increases with an increase in the latter in a non-linearly. It can also be confirmed from the figure that lower temperature of the inlet air favored increase in the final NaOH mass flow rate, as the operation at 373 K produced higher final NaOH mass flow rate than the operation at 382 K, which also produced higher values than those of 391 K as far as their inter-relationship is concerned. This can be explained with fact that at corresponding percent specific energy reduction values, lower temperature will evaporate less moisture from the same quantity of solution, which will in turn result in a final product of higher flow rate but less NaOH concentration.

There is also a justification of significantly statistically wide variation between the experimental final NaOH mass flow rate for various percent specific energy reduction and inlet air temperatures at the 95% confidence interval, based on the Fisher's F and probability factor P values given earlier. The range of values confirmed relationships exists. Based on the information in Tables 1, 2, and 3, the Bonferroni-Holm Posthoc parametric tests for the final NaOH mass flow rate at various percent specific energy reduction at the three operating temperatures further confirmed that they are significant.

3.4. Variation of Specific Energy of Evaporation with final NaOH mass flow rate

From Fig. 5, the variation of the specific energy of evaporation with the final NaOH mass flow rate presented the former as decreasing with an increase in the latter in a non-linear manner.

From the figure, lower temperature of the inlet air increases the specific energy of evaporation with the final NaOH mass flow rate. This is because for a particular value of the mass flow rate of NaOH, lower temperature (energy) will evaporate less moisture from the same quantity of solution, which will in turn result in a final product of higher flow rate but lower NaOH concentration. A significantly statistically wide variation existed between the specific energy of evaporation with final NaOH mass flow rate and inlet air temperatures at the 95% confidence interval, based on the Fisher's F and probability factor P values obtained. The range of values established relationships exists. Based on the

information in Tables 1, 2, and 3, the Bonferroni-Holm Posthoc parametric tests for the specific energy of evaporation with final NaOH mass flow rate at the three operating temperatures confirmed their significance. The highest maximum value of the specific energy of evaporation was 17882.2746 J/kg NaOH, obtained at 373 K, while the lowest minimum value of the specific energy of evaporation was 12493.4951 J/kg NaOH obtained at an inlet air temperature of 391 K.

3.5. Variation of Specific Energy of Evaporation with final NaOH weight percent

As shown in Fig. 6, the variation of the specific energy of evaporation with the final NaOH wt.% presented both parameters increasing with each other in a non-linear manner. Lower temperature of the inlet air increases the specific energy of evaporation. This can be explained with the same phenomenon in Figs. 4 and 5.

A significantly statistically wide variation existed between the specific energy of evaporation with final NaOH wt. % and inlet air temperatures at the 95% confidence interval, as revealed by the Fisher's F and probability factor P values obtained. The range of values established good relationships. Based on the information in Tables 1, 2, and 3, the Bonferroni-Holm Posthoc parametric tests for the specific energy of evaporation with final NaOH wt. % at the three operating temperatures confirmed good significance.

3.6. Variation of Volume Percentage Reduction with specific energy of evaporation

As given in Fig. 7, the variation of the volume percentage reduction with the specific energy of evaporation showed both parameters increasing with each other in a non-linear relationship.

Higher temperature of the inlet air increases the volume percentage reduction with the specific energy of evaporation. This is premised on the fact that more moisture is being evaporated as the temperature increases, which also increases energy used. A significantly statistically variation exists among the volume percentage reduction, specific energy of evaporation and inlet air temperatures at the 95% confidence interval, based on the Fisher's F and probability factor P values. This confirmed relationship exists. Based on the information in Tables 1, 2, and 3, the Bonferroni-Holm Posthoc parametric tests for the volume percentage reduction, specific energy of evaporation at the three inlet air temperatures proved sound significance. The highest maximum value of the volume percentage reduction was 0.9783 obtained at 391 K, while the lowest minimum value of the volume percentage reduction was 0.9545 obtained at an inlet air temperature of 373 K.

3.7. Variation of Volume Percentage Reduction with final NaOH mass flow rate

From Fig. 8, the variation of the volume percentage reduction with the final NaOH mass flow rate showed both parameters displayed a slightly non-linear inverse relationship. Higher temperature.

of the inlet air however resulted in increased volume percentage reduction at corresponding final NaOH mass flow rate. This followed from the same explanation in Fig. 7. Significantly, statistically wide variation exists among the volume percentage reduction, final NaOH mass flow rate and inlet air temperatures at the 95% confidence interval, based on the Fisher's F and probability factor P values. Therefore, relationships exist. From Tables 1, 2, and 3, the Bonferroni-Holm Posthoc parametric tests for the volume percentage reduction, final NaOH mass flow rate at the three inlet air temperatures proved good significance.

4. Conclusion

The performance of the dryer operation with operating conditions within the range of the optimum enabled the achievements of products

and results with some values even exceeding the theoretically predicted values. The model and simulation of the dryer operations showed a high level of accuracy compared to experimental data. The highest final mass flow rate of NaOH with a value of 0.0459 kg/s was 12% higher than the optimum predicted value of 0.040933 kg/s. A maximum value of 73.85% was obtained for the final NaOH wt. %. The optimization technique adopted enabled the achievement of higher productivity of about 400% increase at 73% w/w NaOH product with reduced energy consumption of just 0.086% of that used in another spray dryer operation by Olufemi et al., (2012a). In comparison with the conventional method of using multiple effect evaporators to achieve the same objective (73% w/w NaOH) in this work, improvement on the energy savings was approximately 2.34×10^6 J/kg of energy, which corresponds to about 99.6565% specific energy savings.

Statistical analysis of parameters using ANOVA and the Bonferroni-Holm, Holm-Sidak and Tukey Posthoc parametric tests enabled the confirmation of very sound relationship among the variables involved in the dryer operation. The relative importance and effect of the various parameters were also explored and established. From the results achieved, specific energy reduction tends to be reduced at higher NaOH concentrations, which indicated the energy efficient nature of the operation.

The final mass flow rate of NaOH as depicted in this work is inversely proportional to w/w% NaOH in solution. Improvement in this regard seems possible and therefore recommended for further research.

Possible improvement in the NaOH evaporation operation to achieve better results with the process methodology in order to obtain 100% w/w NaOH product seems achievable and is recommended. Considering, utilizing and optimizing some other parameters not considered in this present work, but which could also be quantified like particle size, atomizer speed, residence time and so on guided by statistical significance can make this a reality.

Declarations

Author contribution statement

Babatope Olufemi, Michael Ayomoh: Conceived and designed the experiments; Performed the experiments; Analyzed and interpreted the data; Contributed reagents, materials, analysis tools or data; Wrote the paper.

Funding statement

This work was supported by the Central Research Committee of the University of Lagos, Nigeria.

Competing interest statement

The authors declare no conflict of interest.

Additional information

No additional information is available for this paper.

Acknowledgements

The University of Lagos through the Department of Chemical and Petroleum Engineering is appreciated for the supportive environment during this work. Ali-Baba Mohammed and Kolawole Olajide are appreciated for helping out during the experimental stage of the work.

References

- Dobry, D.E., Settell, D.M., Baumann, J.M., Ray, R.J., Graham, L.J., Beyerinck, R.A., 2009. A model-based methodology for spray drying process development. *J. Pharm. Innov.* 4 (3), 133–142.

- Djaeni, M., Asiah, N., Suherman, S., Sutanto, A., Nurhasanah, A., 2015. Energy efficient dryer with rice husk fuel for agriculture drying. *Int. J. Renew. Energy Dev.* 4 (1), 20–24.
- Gao, H., Waechter, A., Konstantinov, I.A., Arturo, S.G., Broadbelt, L.J., 2018. Application and comparison of derivative-free optimization algorithms to control and optimize free radical polymerization simulated using the kinetic Monte Carlo method. *Comput. Chem. Eng.* 108, 268–275.
- Ghosh, N., Pal, P.K., Nandi, G., Rudrapati, R., 2018. Parametric optimization of gas metal arc welding process by PCA based Taguchi method on austenitic stainless steel AISI 316L. *Mater. Today: Proc.* 5 (1), 1620–1625.
- Kajiyama, T., Park, K.J., 2010. Influence of air parameters on spray drying energy consumption. *Revista Brasileira de Produtos Agro industriais, Campina Grande* 12 (1), 45–54.
- Kavoshi, L., Hatamipour, M.S., Rahimi, A., 2011. Experimental study of reactive absorption of carbon dioxide in a lab scale spray dryer. *Int. J. Chem. React. Eng.* 9 (A60), 1–13.
- Kwak, D.H., Heo, J.H., Park, S.H., Seo, S.J., Kim, J.K., 2018. Energy-efficient design and optimization of boil-off gas (BOG) re-liquefaction process for liquefied natural gas (LNG)-fuelled ship. *Energy* 148, 915–929.
- McCabe, W.L., Harriot, P., Smith, J.C., 2001. *Unit Operations of Chemical Engineering*, sixth ed. McGraw Hill, New York, pp. 136–145.
- Noh, K., Shin, J., Lee, J.H., 2018. An optimization based strategy for crude selection in a refinery with lube hydro-processing. *Comput. Chem. Eng.* 116, 91–111.
- Olufemi, B.A., Popoola, G., Towobola, O., Awosanya, O., 2012a. Mathematical modelling of a reduced thermal energy consuming spray dryer for evaporating caustic soda solution. *Res. J. Appl. Sci. Eng. Technol.* 4 (11), 1550–1556.
- Olufemi, B.A., Popoola, G.O., Towobola, O.R., Awosanya, O.G., 2012b. Operational characterization of a spray dryer for drying water, caustic soda and sodium chloride solutions. *ARPN J. Eng. Appl. Sci.* 7 (2), 222–228.
- Patel, M.N., 2009. *Process and Energy*, pp. 1–7. <http://www.energymanagertrain-ing.com/announcements/issue27/Winners/MNPatel.doc>. (Accessed 7 January 2010).
- Pinter, J.D., 2007. *Nonlinear Systems Modelling and Optimization Using AIMMS/LGO*, pp. 1–4. http://www.aims.com/aims/download/solvers/aimms_lgo_shortpaper.pdf. (Accessed 21 April 2019).
- Thomas, G.B., Finney, R.L., 1984. *Calculus and Analytic Geometry*. Addison-Wesley Publishing Company, Massachusetts, pp. 1034–1041.
- Tilak, V.B., Orosz, P.J., Sokol, E.A., 2007. Brine Electrolysis. <http://electrochem.cwru.edu/ed/encycl>. (Accessed 13 January 2010).
- Tolmac, D., Prvulovic, S., Dimitrijevic, D., Tolmac, J., 2011. A comparative analysis of theoretical models and experimental research for spray drying. *Mater. Technol.* 45 (2), 131–138.
- Worrel, E., Phylipsen, D., Einstein, D., Martin, N., 2000. Energy Use and Energy Intensity of the U.S. Chemical Industry, pp. 1–40. <http://ies.lbl.gov/iespubs/44314.pdf>. (Accessed 8 January 2011).